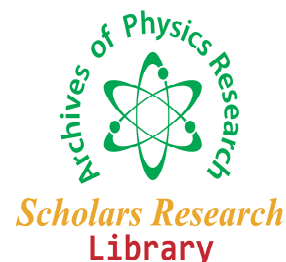




Scholars Research Library

Archives of Physics Research, 2010: 1 (1) 57-66
(<http://scholarsresearchlibrary.com/archive.html>)



Microstructural, Optical and Electrical studies on Sol Gel derived TiO₂ Thin films

S. G. Pawar, S. L. Patil, M. A. Chougule, D. M. Jundhale and V. B. Patil*

Materials Research Laboratory, School of Physical Sciences, Solapur University, Solapur, M.S., India

Abstract

Titanium oxide thin films have been deposited by spin coating technique and then have been analyzed in order to study structural, microstructural, optical and electrical properties. In particular their spectrophotometric and conductivity measurements have been performed in order to determine the optical and electrical properties of titanium oxide thin films. The structure and the morphology of such material have been investigated by SEM, high resolution electron microscopy and small area electron diffraction, AFM.

Keywords: TiO₂, thin films, sol gel, spin coating, XRD, SEM, HRTEM, AFM

Introduction

In recent years, applications of semiconductor metal oxide nanoparticles are getting more extensive covering different fields such as optoelectronics, catalysis, medicine, and sensor devices. Besides, the quantum size effects, the parameters such as structure; size, shape, and elemental composition are considered to be highly important for promising applications of the nanomaterials. Among the metal oxide nanostructures, TiO₂ has extensively been explored for several technological applications such as catalysis, gas sensing, cancer treatment, dye-sensitized solar cells and photonic crystal [1–3]. Such applications of titania have been found to depend strongly on the crystalline structure, morphology, and particle size [4, 5]. On the other hand, the theoretical study and experimental results have shown that the photocatalytic and photovoltaic properties of TiO₂ nanoparticles with two different polymorphic phases (anatase and rutile) are better than pure anatase titanium nanoparticles [6–12]. Mixed-phase TiO₂ material has recently been fabricated by chemical and physical methods, including a sol-gel, hydrothermal, solvothermal, and reactive DC magnetron sputtering method, and has demonstrated excellent

photocatalytic activities [13–15]. As usual, the preparation of titanium nanomaterial with two different polymorphs by sol–gel method needs to crystallize the as-prepared titanium hydroxide at high temperature ($\geq 700^{\circ}\text{C}$). This heat treatment leads to change in the crystallite size as well as morphology of the sol–gel derived titanium oxide [16, 17]. Therefore; the preparation of mixed phase titanium oxide at lower temperature will be useful both in saving energy and in getting better properties. There is no study, known to us, which attempted to prepare TiO_2 biphasic by sol–gel method at lower temperature ($\leq 600^{\circ}\text{C}$).

This paper reports on the investigation of the structural, microstructural, optical and electrical properties of nanocrystalline TiO_2 mix phase (Anatase and Rutile) films prepared by sol-gel method deposited by spin coating.

Materials and Methods

Experimental

The preparation of TiO_2 nanoparticles by sol–gel method has been carried out in several steps and it needs to mix two different solutions. These two solutions are called as precursor and hydrolysis solutions. In our procedure, the precursor solution is a mixture of 5 ml titanium isopropoxide, TTIP (97%, and supplied by Aldrich Chemical) and 20 ml Methanol (99%, supplied by Merck). The hydrolysis solution is a mixture of distilled water and methanol. In order to control the sol–gel reactions (hydrolysis and condensation), different molar ratios of water–methanol have been used as hydrolysis solutions. The pH of hydrolysis solution must be adjusted by HNO_3 acid. Here, we have to emphasize that the preparation of these two solutions is very important and the final results depend highly on the preparation conditions of these starting materials. The gel preparation process was started when the precursor and hydrolysis solutions were mixed together under vigorous stirring at 60°C . After mixing for several minutes, the stirring rate was reduced in order to minimize coagulation of the titanium oxide particles during the sol–gel reactions. The prepared titanium hydroxide was then washed with methanol, dried for several hours at 100°C , and annealed at different temperatures ($400\text{--}700^{\circ}\text{C}$) for 1 h. Powder X-ray diffraction (Philips PW-3710, Holland) instrument was used for crystal phase identification and estimation of the average crystallite size. The (1 0 1) peak of anatase has been considered for crystallite size estimation. High resolution Transmission electron microscopy (HRTEM) and small area electron diffraction (SAED) were obtained in order to investigate the morphology and structure of titanium oxide thin films. The images were taken with a Hitachi Model H-800 transmission electron microscope. In order to determine the particle size and morphology of nanopowder, the calcined samples were dispersed in distilled water and sonicated ultrasonically by using a Cole-Parmer 8851 apparatus, to separate out individual particles. The size and morphology of the powder were then observed on Philips XL 30 scanning electron microscope (SEM). Roughness of the film was determined from the Atomic force microscopy (AFM) using (Digital Instruments) Nanoscope IIIa. Room temperature optical measurements were carried out with a double beam UV-VIS-NIR spectrophotometer using unpolarized light at normal incidence. An integrating sphere was used for reflectance measurements. The resistivity, mobility and carrier concentration of the films were furthermore determined by Hall-effect measurements carried out by the four-point dc Van der Pauw method [18] in a Biorad system.

Results and Discussion

Structural properties

Fig. 1 shows the X-ray diffraction (XRD) pattern of TiO₂ thin film annealed at 700⁰C for 30 min, it is seen that the elaborated TiO₂ thin layer has a nanocrystalline structure and it has been observed in two phases, the anatase phase (A) in which the preferential orientation of crystallites is along the [101] direction, and the apparition of a peaks of rutile phase (R) is at $2\theta = 27.60^{\circ}$, 36.18° , 39.12° .

According to Sabataitytey *et al.* [19], whom used sol-gel method and spray pyrolysis technique for the layer deposition, the obtained structure is anatase at 500⁰C. On the other hand, spin coating [19] technique leads to the formation of the connections of Ti–O–Ti anatase after annealing at 450⁰C; and the rutile crystalline structure was observed after annealing at temperatures higher than 700⁰C.

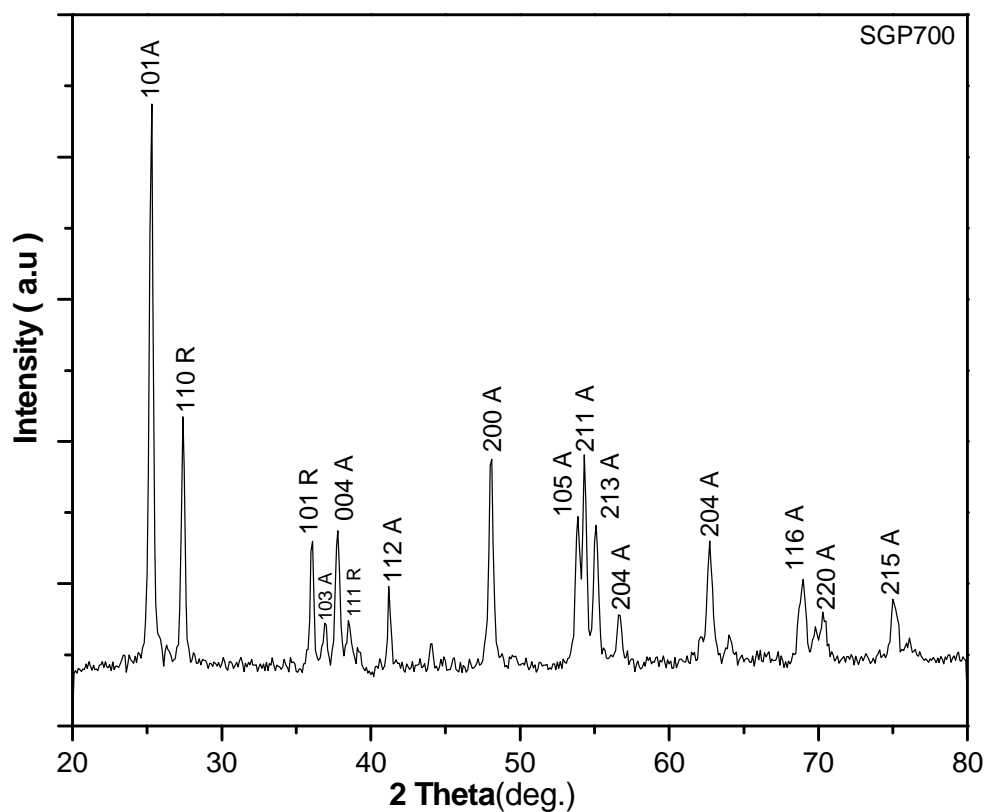


Fig. 1. X-ray diffraction (XRD) pattern of TiO₂ thin film annealed at 700⁰C

Fig. 2 shows the surface morphology of the TiO₂ nanoparticle film, annealed at 700°C for 30 min, has been studied by scanning electron microscopy (SEM). It is clearly observed from the micrograph that the nanoparticles are fine with an average grain size of about 60 nm.

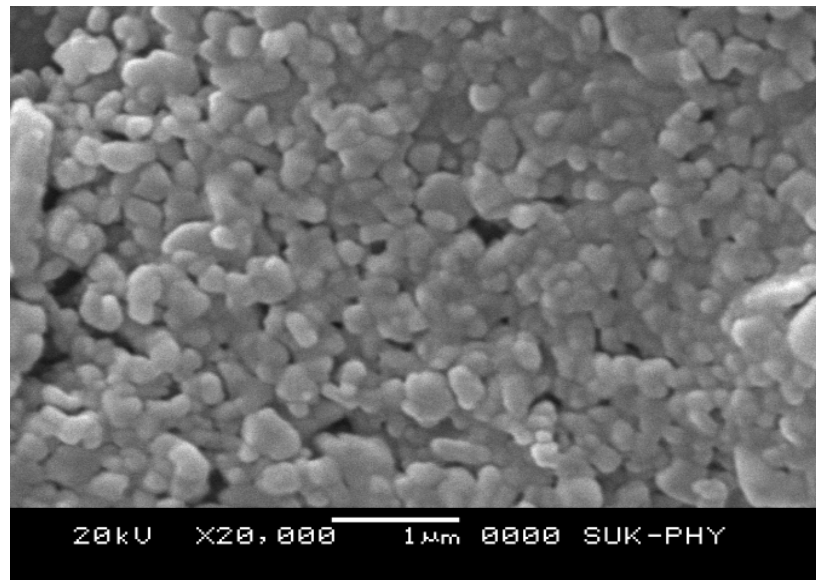


Fig.2. Surface morphology of TiO₂ nanoparticle film annealed at 700°C

Microstructural properties

Figure 3 (a) show high resolution image of titanium oxide thin film annealed at 700°C, recorded from typical regions of films. HRTEM shows a large number of crystalline grains appear in a structured matrix and the grains have a diameter in the range 2–3 nm and show lattice spacings of about 0.35 nm. Figure 3(b) shows the diffraction patterns obtained from the titanium oxide film annealed at 700°C. The different arrangement of dominant diffracted rings indicates a phase evolution of crystalline grains as a consequence of thermal annealing.

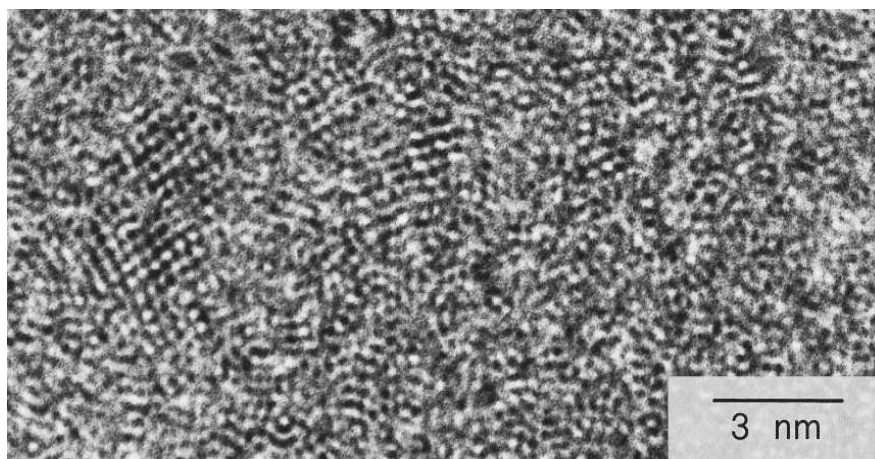


Fig. 3. (a) High resolution TEM image of titanium oxide thin film annealed at 700°C

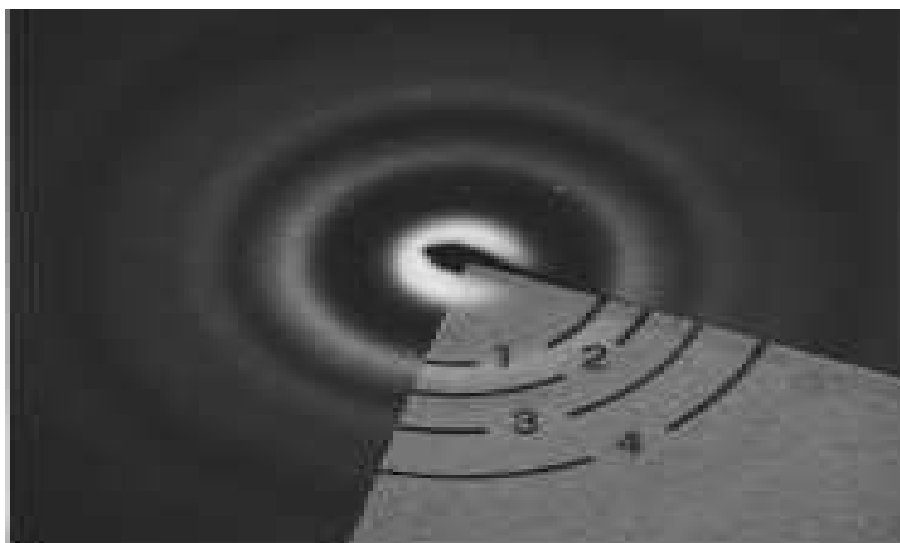


Fig.3. (b) Diffraction patterns recorded on titanium oxide film annealed at 700⁰C

Table I depicts the interplanar spacings determined from diffraction pattern together with the corresponding ones of TiO₂ rutile and anatase phases reported in the literature for comparison. It is evident that the film consists of grains having both the interplanar spacings of TiO₂ in the anatase and rutile structural modifications.

Table I: Interplanar spacings deduced from electron diffraction patterns reported in Fig. 3(b) together with the corresponding ones obtained from literature data. Numbers in brackets (n) represent the labels of reflections in diffraction patterns

Interplanar determined spacings in this work on titanium oxide films		Interplanar spacings reported in literature ^a	
(n)	d (nm)	Rutile d (nm)-hkl	Anatase d (nm)- hkl
(1)	0.3551		0.35126---101
	0.3242	0.3246---110	
		0.25130---101	
(2)	0.2371		0.23775---004
		0.2187----111	
(3)	0.1894		0.18900---200
(4)	0.1665		0.16690---105
			0.16643---211
			0.14754---204

^aJoint commission Powder Diffraction File No. (21-1272 & 21-1276)

AFM (tapping mode) was used to record the topography of the TiO_2 . In this mode, the probe cantilever is oscillated at or near its resonant frequency. The surface morphologies of the TiO_2 NPs exhibit notable features. Figures 5 show 3D AFM images ($20 \mu\text{m} \times 20 \mu\text{m}$) of the TiO_2 NPs films. The average surface roughnesses and peak-to-peak height values are 16, 19 nm for TiO_2 NPs. The average particle sizes of TiO_2 are found to be in the range of 100 ± 50 nm.

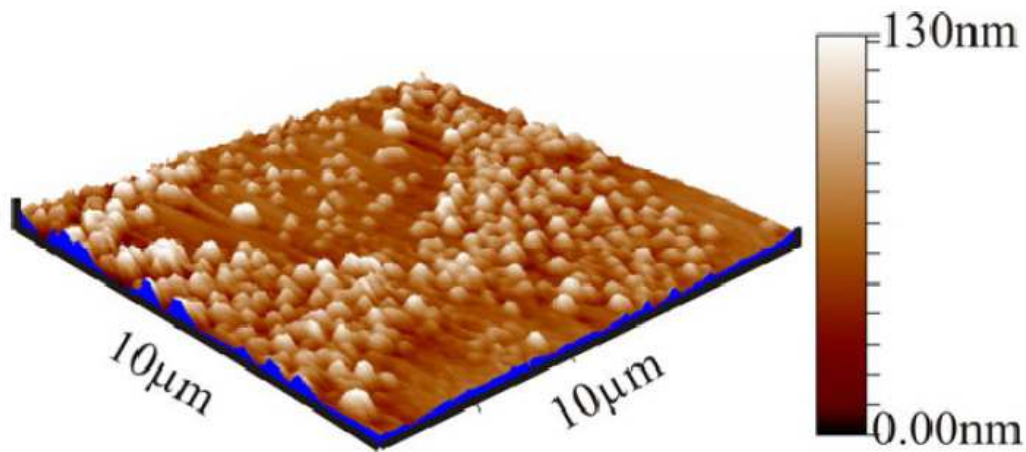


Fig. 4. 3D AFM image of the TiO_2 NPs film

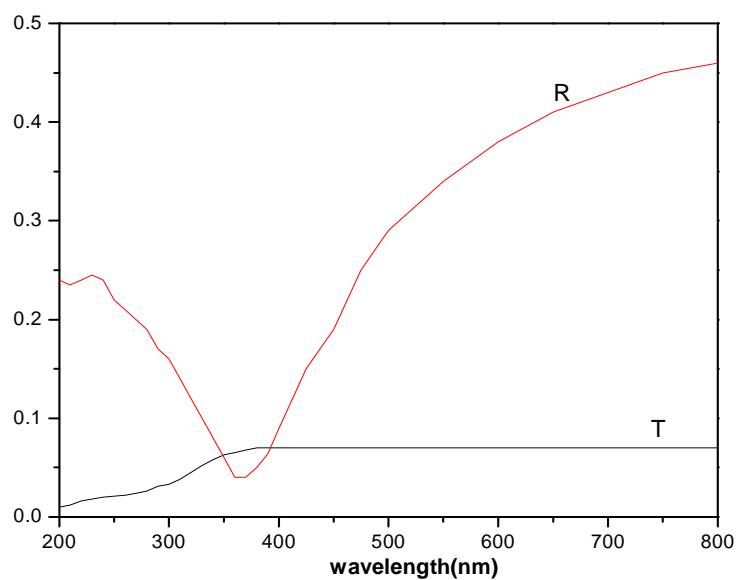


Fig.5. Transmission and Reflection spectra of TiO_2 thin film at 700°C

Optical properties

The analysis of optical transmission spectra is one of the most productive tools for understanding and developing the band structure and energy band gap, E_g of crystalline structure. Figure 5 shows typical transmission and reflection spectra of titanium oxide thin films annealed at 700 °C. The transmittivity of as deposited thin films keeps constant in the investigated range 200–800 nm. A spectrum shows an abrupt decrease in transmission at high energies indicates the onset of interband absorption.

Taking into account multiple internal reflections and neglecting effects of the quartz substrate, the optical absorption coefficient α is given by the following equation [20] as a function of the transmittivity T and reflectivity R:

$$\alpha = \left(-\frac{1}{d} \right) \ln \left\{ \frac{(1-R)^2}{2T} + \left[\left(\frac{(1-R)^2}{2T} \right)^2 + R^2 \right]^{1/2} \right\}, \quad \text{----- (1)}$$

where d is the sample thickness The optical band gap can be determined from the analysis of the spectral behavior near the fundamental absorption edge: Figure 6 shows the variation of the optical absorption coefficient as a function of incident photon energy of titanium oxide thin film annealed at 700 °C . In this case the absorption coefficient α can be written as [21]

$$\alpha h\nu = B(h\nu - E_g)^m, \quad \text{----- (2)}$$

where E_g is the optical band gap corresponding to transition indicated by the value of m . The factor B depends on the transition probability and can be taken constant within the investigated optical frequency range. Let $Y = \alpha h\nu$ and Y' be the first derivative of Y with respect to photon energy, from Eq. (2) one obtains

$$Y/Y' = (h\nu - E_g)/m. \quad \text{----- (3)}$$

Y and Y' are determined from experimental data, m and E_g represent the slope and the intercept of the linear plot Y/Y' versus $h\nu$. Figure 7 shows the plot of Y/Y' as a function of photon energies of titanium oxide thin films annealed at 700 °C. A linear region corresponding to allowed direct transition is evident. From the data of Fig. 7 one obtains $m=1/2$ and an energy gap $E_g = 3.24$ eV. Our experimental results agree with the ones reported in the literature. [22, 23].

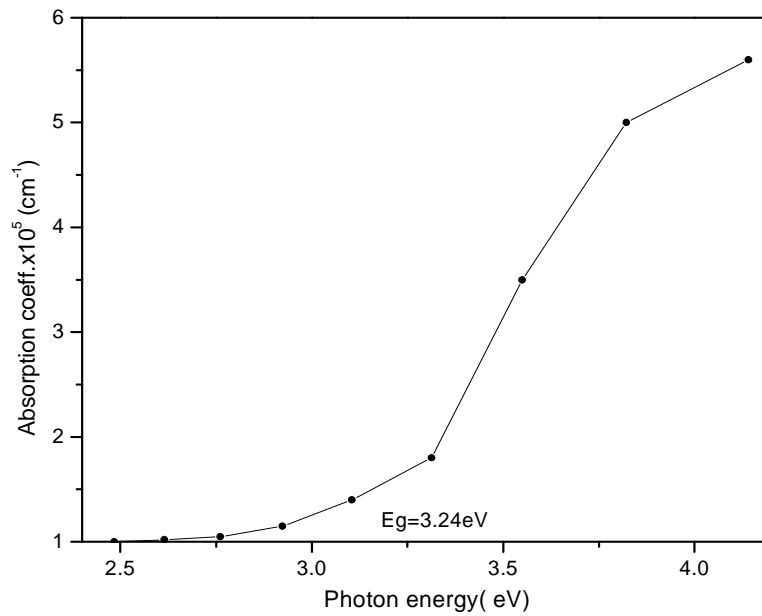


Fig. 6. Variation of the optical absorption coefficient as a function of incident photon energy of titanium oxide thin film annealed at 700°C

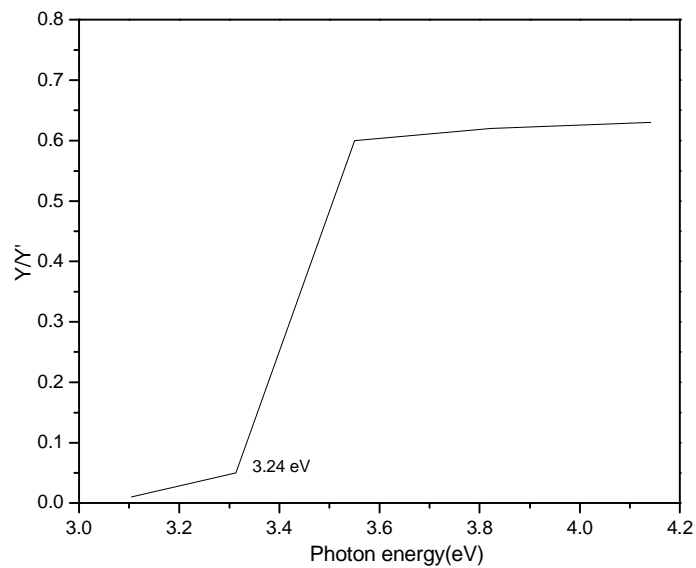


Fig.7. Plot of Y/Y' as a function of photon energies of titanium oxide thin films annealed at 700°C

Electrical properties

With regard to the electrical properties of titanium oxide thin films, Table I reports the experimental data for the electrical resistivity ρ , the carrier density n and the Hall mobility μ of

titanium oxide thin films annealed at 700 °C at room temperature . It is worth stressing that titanium oxide thin films annealed at 700 °C is n-type semiconductors with a free electron density of about $7.7 \times 10^{13} \text{ cm}^{-3}$.

Table II: Electrical resistivity ρ , carrier density n and Hall mobility μ measured at room temperature for as deposited and annealed titanium oxide thin films

Sample	ρ ($\Omega \text{ cm}$)	μ ($\text{cm}^2 \text{ V}^{-1} \text{ s}^{-1}$)	n (cm^{-3})
SGP700	1.4×10^4	5.92	7.7×10^{13}

Conclusion

In summary, TiO₂ thin films have been deposited on a glass/quartz substrate by sol-gel process and spin-coating method and X-ray diffraction shows that it is a nanocrystalline structure. The surface morphology (SEM) of the TiO₂ film showed that the nanoparticles are fine with an average grain size of about 60 nm. HRTEM shows a large number of crystalline grains appear in a structured matrix and the grains have a diameter in the range 2–3 nm with lattice spacings of about 0.35 nm. From electron diffraction pattern it is evident that the film consists of grains having both the interplanar spacings of TiO₂ in the anatase and rutile structural modifications. AFM image showed that the average particle sizes of TiO₂ are in the range of 100 ± 50 nm. An optical transmittance and reflection spectrum shows an abrupt decrease in transmission at high energies indicates the onset of inter band absorption. The electrical study revealed that the titanium oxide thin films annealed at 700 °C is n-type semiconductors with a free electron density of about $7.7 \times 10^{13} \text{ cm}^{-3}$.

Acknowledgments

The author (VBP) thankful to Department of Science and Technology, Government of India, New Delhi for sanctioning Fast Track Project (SR/FTP/PS-09/2007).

References

- [1] T. Thompson, J. Yates Jr., *Chem. Rev.*, **2006**, 106 4428–4453.
- [2] M. Pal, J. Garcya Serrano, P. Santiago, U. Pal, *J. Phys. Chem. C*, **2007**, 111, 96–102.
- [3] S. Ito, T.N. Murakami, P. Comte, P. Liska, C. Grätzel, M.K.Nazeeruddin, M. Grätzel, *Thin Solid Films*, **2008**, 516, 4613–4619.
- [4] H. Lin, C.P. Huang, W. Li, C. Ni, S. Ismat Shah, Y.-H. Tseng, *Appl. Catal. B: Environ.*, **2006**, 68, 1–11.
- [5] B. Gao, Y. Ma, Y. Cao, J. Zhao, J. Yao, *J. Solid State Chem.*, **2006**, 179, 41–48.
- [6] N.A. Deskins, S. Kerisit, K.M. Rosso, M. Dupuis, *J. Phys. Chem. C* 111 (2007) 9290–9298.
- [7] D. Jiang, S. Zhang, H. Zhao, *Environ. Sci. Technol.*, **2007**, 41, 303–308.
- [8] Q. Shen, K. Katayama, T. Sawada, M. Yamaguchi, Y. Kumagai, T. Toyoda, *Chem. Phys. Lett.*, **2006**, 419, 464–468.
- [9] B. Sun, P. Smirniotis, *Catal. Today*, **2003**, 88, 49–59.
- [10] I. Zumeta, R. Espinosa, J.A. Ayllon, X. Domenech, R. Rodriguez-Clemente, E. Vigil, *Solar*

-
- Energy Mater. Solar Cell*, **2003**, 76, 15–24.
- [11] T. Kawahara, Y. Konishi, H. Tada, N. Tohge, J. Nishii, S. Ito, *Angew. Chem. Int. Ed.*, **2002** 41, 2811–2813.
- [12] J.H. Jho, D.H. Kim, S.J. Kim, K.S. Lee, *J. Alloys Compd.*, **2008**, 459, 386–389.
- [13] G. Li, S. Ciston, Z.V. Saponjic, L. Chen, N.M. Dimitrijevic, T. Rajh, K.A. Gray, *J. Catal.*, **2008**, 253, 105–110.
- [14] M. Kanna, S. Wongnawa, *Mater. Chem. Phys.*, **2008**, 110, 166–175.
- [15] H. Choi, Y.J. Kim, R.S. Varma, D.D. Dionysiou, *Chem. Mater.* **2006**, 18 377–5384.
- [16] N. Wetchakun, S. Phanichphant, *Curr. Appl. Phys.*, **2008**, 8, 343–346.
- [17] H.I. Hsiang, S. C. Lin, *Ceram. Int.*, **2008**, 34, 557–561.
- [18] L. J. Van der Pauw, *Philips Res. Rep.*, **1958**, 13, 1-15.
- [19] J. Sabataityte, I Oja, F. Lenzmann, O. Volobujeva, M. Krunks, *Comptes Rendus Chimie* **2006**, 9, (5–6) 708–712.
- [20] T. S. Moss, *Optical Properties of Semiconductors*- Butterworth's, London, **1979**.
- [21] G. Burns, *Solid State Physics*- Academic, New York, **1985**.
- [22] A. Amtouth and R. Leonnel, *Phys. Rev. B*, **1995**, 51, 6842-6853.
- [23] K. M. Glassford and J. R. Chelikowsky, *Phys. Rev. B*, **1992**, 46, 1284-1290.